Effects of adding graphene nanoparticles in decreasing of residual stresses of carbon/epoxy laminated composites

M.M. Shokrieh* and M. Shams Kondori[a]

Composites Research Laboratory, School of Mechanical Engineering, Iran University of Science and Technology, Narmak, 16846-13114, Tehran, Iran

Abstract. In the present paper, changes in the residual stress of carbon/epoxy laminated composites as a result of adding graphene nanoparticles (GNPs) content were studied theoretically and experimentally. Three dissimilar weight fractions of GNPs, i.e., 0.1%, 0.25% and 0.5%, were added into an epoxy matrix. Unidirectional carbon fibers (CFs) were used as reinforcement to fabricate cross-ply laminated composites. Mechanical and thermal properties of the GNP/epoxy nanocomposites were then characterized via tensile tests as well as thermomechanical analysis (TMA). Based on experimental observations, adding even small fractions of GNP to epoxy matrix caused to decrease in the coefficient of thermal expansion (CTE) significantly while the epoxy resin Young's modulus increases moderately. The measurements of residual stresses in cross-ply CF/epoxy and GNP-CF/epoxy laminated composites were performed using the slitting method. The results of experiments show 11.7%, 14.3% and 16.52% reductions in residual stresses as a result of adding 0.1%, 0.25% and 0.5% GNP to the matrix of the cross-ply CF/epoxy laminated composites, respectively. This is conclusive evidence that GNP can reduce CTE and decrease residual stresses significantly.

Keywords: laminated composites; residual stresses; polymer; graphene nanoparticles; Coefficient of thermal expansion; Young's modulus

1. Introduction

In the curing process, when the temperature of carbon fiber composites is reduced from the curing temperature to the environment temperature, CTE of a polymer matrix causes a significant contraction. On the contrary, the contraction in carbon fibers (CFs), which have a low CTE, under similar temperature changes is negligible. This contrast in thermal behavior between the matrix and CF is the main reason for the creation of residual stresses which critically reduce the performance and strength of the laminated composites. The negative consequences include premature failure, warpage, cracking, and delamination Hodges *et al*. (1989), Gascoigne (1994), Brown *et al*. (2019). A similar behavior can be observed in the tire material production. In the study by Liang *et al*. (2020), the effect of change at Young's Modulus the tire's behavior has been presented. Addressing these significant problems requires the development of techniques to limit the residual stresses.

*Corresponding author, Professor, E-mail: Shokrieh@iust.ac.ir
[a]Ph.D. Student, E-mail: Mehran@vt.edu

Previous methods have modified curing cycles with limited success.

Furthermore, the advent of negative thermal expansion materials has proved advantageous in these applications Kim *et al*. (2013). Parhizkar *et al*. (2016) studied the effects of glass fibers and CaCO$_3$ nanoparticles on mechanical and heat performances of homo-PP based composites. Elastic properties of CNT- and graphene-reinforced nanocomposites using RVE studied by Kumar *et al*. (2016). According to Takenaka (2012), such materials could compensate for the undesirable consequences of thermal expansion differences. Along the same lines, in order to fabricate adjustable thermal expansion composites, one could potentially incorporate negative CTE nanoparticles into a polymer. Graphene nanoplates (GNPs) and carbon nanotubes (CNTs) are two instances of negative thermal expansion nanoparticles that have been proved to be helpful in decreasing the residual stresses in laminated polymer composites Shokrieh *et al*. (2013). These thermal residual stresses in laminated composites are primarily governed by CTE and Young's modulus of composite elements. Since graphene nanoparticles have significantly lower CTE and higher Young's modulus, as compared with the polymer matrix, dispersion of such nanoparticles into the polymer matrix would make its specification closer to those of the fiber itself Nishino *et al*. (2009), Wang *et al*. (2007). Therefore, by adding these nanoparticles to the matrix the residual stress can be reduced in laminated fibrous composites. Moreover, the addition of nanoparticles improves the dimensional stability of the composite components, as demonstrated by Badrinarayanan *et al*. (2012), Cheng and Finnie (2007). other studies have been explored implementing carbon Nano tubes to study and improve mechanical properties of composites using finite element modeling and experimental approaches Hajilounezhad *et al*. (2018).

Shokrieh *et al*. (2013) studied the effects of carbon nanofibers (CNFs) on residual stresses in CF/epoxy laminated composites. In that study, residual stresses in the CNF/carbon/epoxy laminated composites were reported to reduce by 4.4%, 18.8%, and 25.1% following the addition of 0.1 wt.%, 0.5 wt.%, and 1 wt.% of carbon nanofibers, respectively. The effects on the ply-level thermal residual stresses in CF/epoxy laminated composites due to the addition of GNPs are investigated in the present study. Thermomechanical analysis (TMA) was used to measure the CTE of 0.5 wt.% GNP/epoxy composites as well as the neat epoxy. The slitting method, also known as the crack compliance method, Chitsazzadeh *et al*. (2011) was utilized to evaluate and quantify the effects of GNP on the residual stresses, specifically in the cross-ply CF/epoxy and GNP/CF/epoxy laminated composites. The experiments demonstrated a substantial decrease in residual stresses in carbon/epoxy laminated composites as the GNP weight fraction increased.

2. Experimental method

GNP/epoxy composites and GNP/CF/epoxy composites were fabricated and characterized. GNP particles with weight fractions of 0.1 wt.%, 0.25 wt.%, and 0.5 wt.% were dispersed into the epoxy matrix. The epoxy matrix was then reinforced with carbon fibers. The residual stresses in these laminates were measured using the slitting methods. The following sections cover the details of the experimental setup and methodology.

2.1 Materials

The laminates were fabricated using ML-506 (Mokarrar Engineering Materials, Tehran, Iran) and Aradur-830 (Huntsman, Säckingen, Germany) with a ratio of 100:60. Table 1 presents the

Table 1 Characteristics of carbon fibers

	Type	Manufacturer	E (GPa)	CTE (10^{-6}/°C)
Carbon fibers	T300, 12k, UD	Toray	182	Longitudinal, -1.5 Transverse, +1.5

characteristics of carbon fibers.

A grade-M particle-based GNP with an average thickness of 6-8 nanometers, a typical surface area of 120-150 $\frac{m^2}{g}$ and 15 μ diameter has been used in this study. Unidirectional T300 carbon fibers (Toray, Tokyo, Japan) were used to fabricate the unidirectional ply and cross-ply laminates.

2.2 Samples fabrication

Pre-calculated amounts of ML-506 epoxy were mixed with Ardur-830 curing agent to prepare the neat resin specimen. A two propelled stirrer was used to stir the mixture constantly for a duration of 30 minutes at 2000 rpm. The air bubbles were then removed via putting the mixture in a vacuum for 30 minutes. Next, the sonication technique was used to fabricate the GNP/epoxy composite specimen reinforced with three different GNP weight fractions. This procedure started with mixing the resin with the desired GNP contents under a 2000 rpm consistent stir for 30 minutes. Consequently, a Sonicator (Hielscher UP400S, Teltow, Germany) at 200 W with a probe of 14 mm diameter was used to sonicate the mixture. The mixtures of epoxy resin and GNP with 0.1, 0.25, 0.5 wt.% GNP content were sonicated for 40, 60, 80 minutes, respectively, under consistent ice-bathing, to achieve homogeneity Chitsazzadeh *et al.* (2011). Following sonication, the curing agent was added while the mixture was being stirred at 250 rpm, a process which completed in 20 minutes. Again, degassing in a vacuum chamber for 30 minutes was used to get rid of any air bubbles. Eventually, the resulting pure resin and GNP/epoxy mixtures were poured into steel molds. These mixtures were then cured for 6 hours at 100°C and subsequently, for another 6 hours at 120°C. The release of the cured specimens was facilitated with a mold-release agent which was added on top of the mold surface. This process was followed by a free cooling to room temperature. The hand lay-up method was used for fabricating three-phase composites GNP/CF/epoxy. The GNP required for the three-phase GNP/CF/epoxy composite was manufactured in a procedure identical to that of producing the two-phase GNP/epoxy composites.

Eventually, the composite was manufactured by the hand lay-up method after adding the curing agent to the GNP/epoxy mixture. Moreover, the curing process for the three-phase composites was similar to the method for two-phase composites. The process of laminating was performed on a steel plate. In order to facilitate demolding of the cured laminate, the steel plate was waxed prior to the lamination. The entrapped air bubbles were removed using a roller which also helped to spread the resin uniformly between different layers. An oven was used to cure the laminated composite plate. The fiber volume fraction of CF in the final laminates was approximately 50% for all composite specimens.

2.3 Thermomechanical characterization

The tensile test as per ASTM D638-Type I (1997) were used to measure Young's modulus of the fabricated GNP/epoxy specimens. A universal testing apparatus (STM-150, Santam, Iran) with a 50

Fig. 1 Pure epoxy and GNP/epoxy samples fabricated for tensile tests
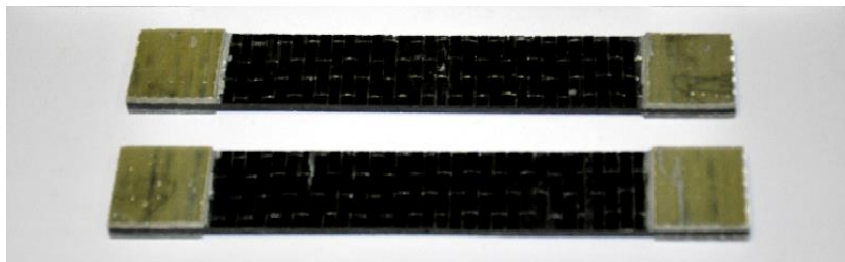
Fig. 2 Unidirectional samples of GNP/CF/epoxy composites (in both directions of longitudinal and transverse) used for tensile tests

kN load cell was used under displacement control mode and at a crosshead speed of 1.0 mm/min to perform the tensile tests. The strain measurement was performed using an extensometer tensile test with a 50 mm gage length. Pneumatic grips with an inter-grip distance of 40 mm were used to clamp each specimen under the test. Mechanical polishing to minimize surface flaws, including porosity, was performed before the tensile tests. For each GNP content percentage, at least five samples were tested, with the final characterization being the average of the five experiments. Fig. 1 presents the pure epoxy and GNP/epoxy samples fabricated for the tensile tests. The samples have an overall length of 165 mm, an overall width of 19 mm, a thickness of 3.2 mm, a gage width of 13 mm, and a gage length of 50 mm.

The compliance coefficients are required for residual stress determination. These compliance coefficients, in turn, require the knowledge of Young's modulus of unidirectional GNP/CF/epoxy composites. Static strength tests, as per ASTM D3039 (1997), were performed on the unidirectional GNP/CF/epoxy three-phase composites, in both longitudinal and transverse directions. The 0-degree unidirectional specimens were about $250 \times 15 \times 1.2$ mm in dimensions, whereas the 90-degree unidirectional specimens were approximately $175 \times 25 \times 2.1$ mm. Fig. 2 presents two 0-degree and 90-degree unidirectional samples.

Experiments were performed on three specimens for each GNP composites (for each weight fraction). A comparison between the CTE of the pure resin and that of the GNP/epoxy specimens

Fig. 3 PL-TMA CTE measurement device (Iran Polymer and Petrochemical Institute)

via the TMA was used to study the effects of GNP on CTE of epoxy. The CTEs were measured as per ASTM E831-14 (2014), i.e., it was calculated as the ratio between the slope of the thermal strain and temperature curve:

$$\alpha = \frac{\Delta L}{L_0 \Delta T} \tag{1}$$

where ΔL is the heating-induced change in composite length, L_0 is the initial length, and ΔT is the temperature difference.

The residual stresses are primarily due to the difference between the thermal expansion coefficient of fibers and matrix. Thermal expansion coefficients of GNP/epoxy composites with various weight percentages of GNP were obtained experimentally. Then, fiber thermal properties and the rule of the mixture were used to calculate the longitudinal as well as the transverse thermal expansion coefficients of an orthotropic layer. The required GNP/epoxy nanocomposites were fabricated by the method explained in section 2.2 of the present paper. Thermal expansion coefficients were measured as per the ASTM-E831-14 (2014) TMA method. The device used for the TMA measurements is depicted in Fig. 3.

A thermo-mechanical analyzer (TMA-120, Seiko Instruments, Tokyo, Japan) was used to carry out the TMA. The test specimen dimensions were 5×7×7 mm. A constant heating rate of nearly 0.1°C/s was applied at an ambient temperature of 140°C. Measuring the CTE of GNP/epoxy composites at three different weight fractions of 0.1 wt.%, 0.25 wt.%, and 0.5 wt.% allowed for evaluating the effects of adding GNP content.

2.4 Experimental study

The slitting method is a well-developed and trustworthy method prevalently used to measure the
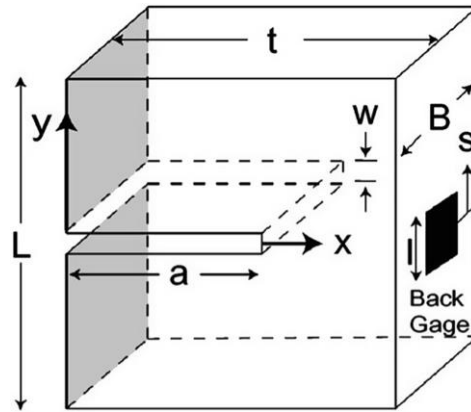
Fig. 4 Schematic of the slitting method Lee MJ (2007)

residual stress in various engineering materials. This method was used by Hill (2002), Lee (2007a) to measure the residual stresses of polymeric laminated composites. The slitting method enables stress measurement not only at the surface but also at the subsurface levels of stressed components. Conventionally, a narrow slit is cut in successive increments in one surface of the specimen; then, a strain gage bonded to the other surface is used to measure the strains by Lee (2007b), Zuccarello (1999). Fig. 4 demonstrates the slitting method.

2.4.1 The slitting method

The slitting method was used for measuring the residual stresses in GNP/CF/epoxy composite samples with $[0_4/90_4]_s$ lay-up. Five samples were tested for each weight fraction of GNP. Specimens used in the slitting experiment were 60×20×4.8 mm in dimensions. The equality of depth increments of the slits cut in the specimen plays a significant role in the reliability of the residual stress measurements obtained using the slitting method. Therefore, a computer numerical control (CNC) milling machine (PC Mill 155, EMCO Maier, Hallein, Austria) was used to carry out the slitting experiments (Fig. 5). This ensures the accuracy of slit depth measurements. The specimen was clamped on the end furthest from the slit and gage. The other end of the specimen was unconstrained, so it could undergo free deformations, thus ascertaining the accuracy of strain measurements. A circular cutter with a rotational speed of 5000 rpm, a thickness of 0.2 mm, and a diameter of 23 mm was used. Slitting started at the surface of each specimen in the longitudinal direction (fiber direction) of the first layer. The relative position of the strain gage and cutter are demonstrated in Fig. 4. Furthermore, a single element strain gage (UBFLA-03, TML, Tokyo, Japan) with a gage length of 0.3 mm was used to measure the strains associated with the incremental slitting. The small size of the gage guarantees a minimum error in strain averaging and high precision in any location. The Lakhild 495 adhesive (Tokyo, Japan) was used to bond the strain gages. Prior to bonding, acetone was used to de-grease specimen surfaces. The strain gage must be bonded directly opposite to the slit. This marks the maximum deformation on the surface and the strain amplitude significantly declines if the strain gage departs this location. The alignment accuracy is also imperative in ensuring accurate measurements.

Finally, a computerized system was used to acquire data from the strain gage through a direct connection using a three-wire temperature-compensating circuit. The main liability to error in residual stress measurement is the strain measurement procedure. Thermal-induced strains, as well

Fig. 5 Experimental setups of the slitting test

as machining-induced strains and instrumentation errors, are the primary sources of measurement noise. Furthermore, a reduced number of steps in calculation tends to increase the sensitivity of results to measurement errors. Therefore, using a great quantity of strain data will introduce instability in results Zuccarello (1999). Hence, the number of depth increments was limited to eight with the slitting in successive depth increments of 0.3 to 2.4 mm. The latter corresponds to a depth of half of the specimen thickness. The depth increment was equal to the thickness of each layer of the laminate. The cutter was taken out of the specimen and stopped at the end of each slitting step. This was followed 3 minutes later by a strain measurement step. This delay was designed to allow for an attenuation of any temperature changes due to the slitting procedure.

2.4.2 The eigenstrain method

The calibration coefficients required to convert strains to residual stresses were obtained using the eigenstrain method. In short, thermal stresses were taken into account to calculate the eigenstrain and then, the residual stress was calculated based on equations presented in Shokrieh *et al*. (2013).

2.4.3 The finite element modeling

Finite element simulations formed the basis of calculating compliance coefficients. This approach has been used to model different materials and to solve different problems in Engineering. The type of the elements can be chosen according to the different types of loadings that are applying on the model and its material properties. For example, to model the composite materials that have been used for tire modeling, to capture the torsion of the rubber, 4-Node axisymmetric elements have been used Liang *et al*. (2020), Mashadi *et al*. (2015). In this study, the 8-node 3-D layered elements, Solid46, were used to construct the mesh. In order to accommodate the significant variations in stress and strain, the mesh was then refined towards the slit location, as displayed in Fig. 6. The element spacing in the z-direction was uniform, i.e., equal spacing. In the experimental setup, one end of the sample was clamped. The finite element method was based on the empirical values for the elastic constants of GNP/CF/epoxy composites.
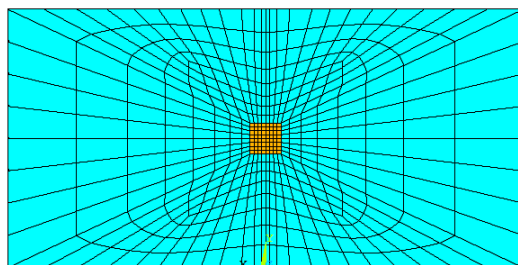
Fig. 6 The bottom view of the finite element model of the specimen

Table 1 Young's modulus of the pure polymer, GNP/epoxy nanocomposites, CF/Epoxy unidirectional composites and GNP/CF/Epoxy unidirectional composites with three different weight fractions of GNP

GNP (wt.%)	Young's modulus (GPa)		
	E	E_x	E_Y
0	2.51	92.25	4.95
0.1	2.74	92.37	5.39
0.25	2.93	92.46	5.76
0.5	2.95	92.47	5.80

where E is the matrix Young's modulus, E_x is Young's modulus in the longitudinal direction and E_y is the transverse Young's modulus.

The slitting process was simulated stepwise wherein each step, the elements at the slitting area were removed, loads were applied on the slit boundary elements, and then, the strain at each strain gage position was calculated. The node displacements for those nodes on the gage borders as well as the gage length were the parameters to determine the simulated gage strain, Schajer (1993).

3. Results and discussion

3.1 Effects of GNP on Young's modulus of GNP/epoxy composites

The average tensile test results for all three types of composites as well as the results for the pure resin are delineated in Table 1.

The average slope of the stress-strain curves in the linear region was used to represent Young's modulus of each specimen. The results indicate that GNP dispersion into epoxy has a moderate effect on Young's modulus of the two-phase composites. A 17% increase in Young's modulus of GNP/epoxy nanocomposites was observed as compared to the neat resin.

3.2 Experimental results for CTE using TMA

Fig. 7 presents the coefficients of the linear thermal expansion of GNP/epoxy nanocomposite samples fabricated in this study obtained by TMA tests. The CTE values for the GNP/epoxy nanocomposite specimens at three different weight fractions as well as those of the neat epoxy measured at room temperature are reported in Fig. 7. A significant decrease in all CTE values
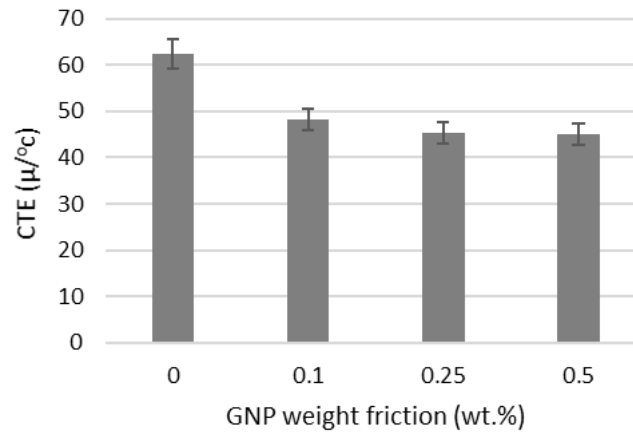
Fig. 7 Experimental coefficients of thermal expansion of GNP/epoxy nanocomposites
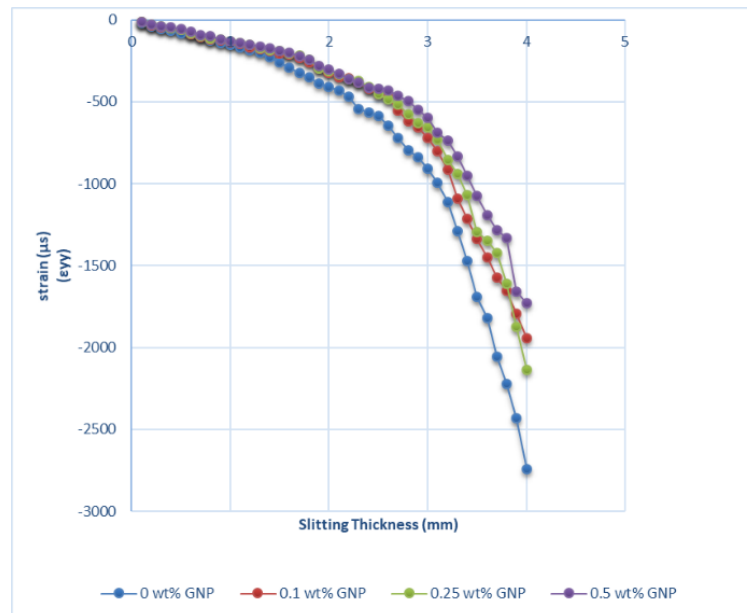
Fig. 8 Strain (µɛ) measurements in GNP/CF/epoxy composite samples of different GNP weight fractions under the slitting test

corresponds to the increase in the weight fraction of the GNP constituent. This result is in line with expectations as the CTE value of GNP is much less than that of the neat epoxy. As shown in Fig. 7, CTE reduced by 22.7%, 27.3%, and 27.9% for the GNP weight fractions of 0.1, 0.25, and 0.5 wt.%, respectively.

Characterization tests, however, demonstrated that the effects of adding GNP to epoxy on Young's modulus of the matrix are in fact negligible. Nevertheless, CTE of the nanocomposites is significantly affected by adding GNP. The incentives for modification of thermomechanical properties of polymers by adding nanoparticles such as CNT are extensively studied previously by Shokrieh (2013). In short, the large interfacial area between the nanoparticle and the matrix, a strong

interface bonding, and a good impregnation of the matrix with the nanoparticle would be the major factors contributing to significant CTE reduction in polymers reinforced with nanoparticles.

The Young's modulus of CF is 230 GPa and the CTE is 0.41×10^{-6} 1/°C as per the CF data sheet provided by Toray Co., whereas Young's modulus of the neat epoxy is 3.13 GPa and the CTE is 63.46×10^{-6} 1/°C. As a result, the reduction of matrix CTE has a direct relation to any reduction in the residual stresses in GNP/CF/epoxy composites.

3.3 Results obtained for residual stress in GNP/CF/epoxy composites

As mentioned before, three different samples of each composite specimen were tested using the slitting method. Fig. 8 presents the average strains measured during the slitting experiments. It was observed that increased GNP weight fraction is correlated with decreased strains.

As shown in

Table 2, strain measurements increased with slit depth. Slitting the specimen would be continuing until the half of the thickness due to the symmetric layup of composites.

Table 2 Average strain ($\mu\mathcal{E}$) measurements in GNP/CF/epoxy composite samples of different GNP weight fractions

Slit depth (mm)	GNP (wt.%)			
	0	0.1	0.25	0.5
0.0	0	0	0	0
0.3	-56	-47	-40.5	-39
0.6	-90	-85	-81	-70
0.9	-140	-123	-120	-118
1.2	-186	-169	-154	-152
1.5	-259	-203	-192	-190
1.8	-241	-243	-254	-351
2.1	-330	-336	-348	-433
2.4	-416	-410	-420	-563
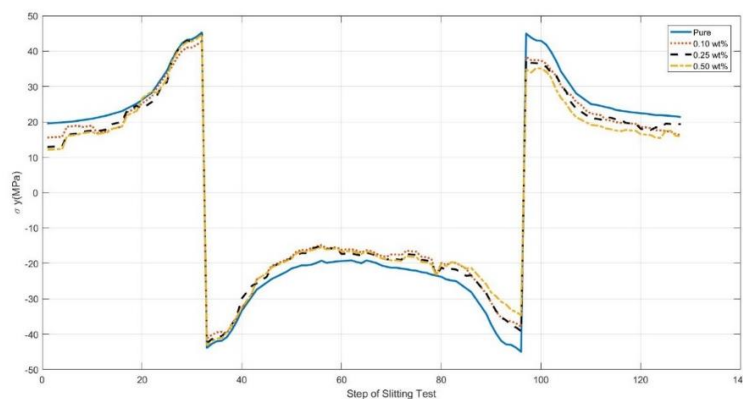
Fig. 9 Residual stress (MPa) distribution in different steps of slitting test at $[0_4/90_4]_s$ composites, for three different GNP weight fractions

The residual stresses obtained by experiments, presented in Fig. 9, are tensile in the 0º layers and compressive in the 90° layers. It was observed that increasing GNP content is accompanied by decreased residual stress in almost all layers. Generally, the layers with higher residual stress experience a more dramatic change in their residual stress. The residual stresses of 0.5 wt.% GNP/CF/epoxy composite are approximately 16.52% less than the CF/epoxy composite. Not only the GNP addition decreases the residual stress in general, but it also results in a more uniform stress distribution as well which in turn reduces the stress concentration across layer boundaries. This effect is demonstrated in Fig. 9.

4. Conclusions

The difference between the coefficient of the thermal expansion (CTE) of fibers and the matrix can be reduced by using low CTE nanoparticles as thermal expansion compensators. Following the addition of such nanoparticles to the matrix of polymeric laminated fibrous composites, thermal residual stresses can be reduced. The graphene nanoparticle (GNP), with a significantly larger Young's modulus and considerably lower CTE compared with the epoxy, is a particularly suitable option. The CTE of CF/epoxy composite was shown to reduce by 27.9% with a 0.5 wt.% GNP addition as measured by the TMA. Furthermore, a moderate increase in Young's modulus of the epoxy matrix due to the GNP loading was a concomitant observation. The slitting method was used to measure the residual stresses of three-phase GNP/CF/epoxy composites. The results demonstrated a 11.7%, 14.3% and 16.52% reduction in residual stress corresponding to 0.1, 0.25, and 0.5 wt.% GNP loading. Further increases in GNP weight fraction are expected to further decrease the residual stresses. The current results demonstrate the decrease of residual stresses of the laminated composites as a consequence of adding GNP to CF/epoxy composites which are comparable to the effects of CNF addition to CF/epoxy presented in Shokrieh *et al*. (2013). Therefore, Nano-particles with negative thermal expansion significantly reduces the thermal residual stresses in fiber-reinforced composites.

References

ASTM D 3039-95 (1997), Standard Test Method for Tensile Properties of Fiber-Resin Composites, Philadelphia, 1993 Annual Book ASTM Standards, PA.

ASTM E831-14 (2014), Standard Test Method for Linear Thermal Expansion of Solid Materials by Thermomechanical Analysis, West Conshohocken, ASTM International, PA.

Badrinarayanan, P., Rogalski, M.K. and Kessler, M.R. (2012), "Carbon fiber-reinforced cyanate ester/nano-ZrW$_2$O$_8$ composites with tailored thermal expansion", *ACS Appl. Mater. Interf.*, **4**(2), 510-517.

Cheng, W. and Finnie, I. (2007), *Residual Stress Measurement and the Slitting Method*, Springer Science and Business Media.

Chitsazzadeh, M., Shahverdi, H. and Shokrieh, M.M. (2011), "Fabrication of multi-walled carbon nanotube/vinyl ester nanocomposites: dispersion and stabilization", *Defect Diffus. Forum*, **312**, 460-465.

Gascoigne, H.E. (1994), "Residual surface stresses in laminated cross ply fiber-epoxy composite materials", *Exp. Mech.*, **34**(1), 27-36.

Hajilounezhad, T. and Maschmann, M.R. (2018), "Numerical investigation of internal forces during carbon nanotube forest self-assembly", *Proceedings of the ASME 2018 International Mechanical Engineering Congress and Exposition*, **2**, Advanced Manufacturing, ASME.

Hill, M.R. and Lin, W.Y. (2002), "Residual stress measurement in a ceramic-metallic graded material", *J. Eng. Mater. Technol., Tran. ASME*, **124**(2), 185-191.

Hodges, J., Yates, B., Darby, M.I., Wostenholm, G.H., Clemmet, J.F. and Keates, T.F. (1989), "Residual-stresses and the optimum cure cycle for an epoxy-resin", *J. Mater. Sci.*, **24**(6), 1984-1990.

Brown, J., Hajilounezhad, T., Dee, N.T., Kim, S., Hart, A.J. and Maschmann, M.R. (2019), "Delamination mechanics of carbon nanotube micropillars", *ACS Appl. Mater. Interf.*, **11**(38), 35221-35227.

Kim, H.S., Yoo, S.H. and Chang, S.H. (2013), "In situ monitoring of the strain evolution and curing reaction of composite laminates to reduce the thermal residual stress using FBG sensor and dielectrometry", *Compos. Part B-Eng.*, **44**(1), 446-452.

Kumar, D. and Srivastava, A. (2016), "Elastic properties of CNT-and graphene-reinforced nanocomposites using RVE", *Steel Compos. Struct.*, **21**(5), 1085-1103.

Lee, M.J. and Hill, M.R. (2007), "Effect of strain gage length when determining residual stress by slitting", *J. Eng. Mater. Technol., Tran. ASME*, **129**(1), 143-150.

Lee, M.J. and Hill, M.R. (2007), "Intralaboratory repeatability of residual stress determined by the slitting method", *Exp. Mech.*, **47**(6), 745-752.

Liang, C., Ji, L., Mousavi, H. and Sandu, C. (2020), "Evaluation of tire traction performance on dry surface based on tire-road contact stress", *SIAR International Congress of Automotive and Transport Engineering*: 138-152.

Mashadi, B., Mousavi, H. and Montazeri, M. (2015), "Obtaining relations between the Magic Formula coefficients and tire physical properties", *Int. J. Autom. Eng.*, **5**(1), 911-922.

Nishino, T., Kotera, M. and Sugiura, Y. (2009), "Residual stress of particulate polymer composites with reduced thermal expansion", *J. Phys.: Conf. Ser.*, **184**(1), 012026.

Parhizkar, M., Shelesh-Nezhad, K. and Rezaei, A. (2016), "Mechanical and thermal properties of Homo-PP/GF/CaCO$_3$ hybrid nanocomposites", *Adv. Mater. Res.*, **5**(2), 121-130.

Schajer, G.S. (1993), "Use of displacement data to calculate strain gage response in non-uniform strain fields", *Strain*, **29**(1), 9-13.

Shokrieh, M.M., Daneshvar, A., Akbari, S. and Chitsazzadeh, M. (2013), "The use of carbon nanofibers for thermal residual stress reduction in carbon fiber/epoxy laminated composites", *Carbon*, **59**, 255-263.

Takenaka, K. (2012), "Negative thermal expansion materials: Technological key for control of thermal expansion", *Sci. Technol. Adv. Mater.*, **13**(1), 013001.

Wang, S., Liang, Z., Gonnet, P., Liao, Y.H., Wang, B. and Zhang, C. (2007), "Effect of nanotube functionalization on the coefficient of thermal expansion of composites", *Adv. Funct. Mater.*, **17**(1), 87-92.

Zuccarello, B. (1999), "Optimal calculation steps for the evaluation of residual stress by the incremental hole-drilling method", *Exp. Mech.*, **39**(2), 117-124.

CC